Mechanical Properties and Morphology of Melt-mixed PA6/SWNT Composites: Effect of Reactive Coupling

Arup R. Bhattacharyya,[*1] *Petra Pötschke*[2]

Summary: An interfacial reaction during melt mixing of maleic anhydride copolymer (SMA) encapsulated single wall carbon nanotubes (SWNT) and polyamide 6 (PA6) was used in order to disperse SWNT homogeneously and to enhance interfacial adhesion. The intended reactive coupling between PA6 and SMA was evident from IR spectroscopy. Nanocomposites with SMA encapsulated SWNT showed increased elongation at break as compared to PA6/SWNT composites. SEM investigation of tensile fractured surfaces of PA6/SWNT+SMA composites indicated enhanced interfacial adhesion between PA6 and SMA modified SWNT.

Keywords: Morphology; nanocomposites; polyamide 6; reactive processing; single wall carbon nanotubes

Introduction

Carbon nanotubes (CNT) based polymer composites have attracted considerable attention in the scientific and industrial community due to the possibility to exploit the unique properties of CNT.[1,2] Several studies have been reported to reinforce polymer matrices where either single wall carbon nanotubes (SWNT) or multiwall carbon nanotubes (MWNT) were introduced into the polymer matrices by several mixing techniques. These include the utilization of in-situ polymerization, mixing of polymer solutions or melt mixing to produce polymer/CNT composites e.g., PBO/SWNT, PP/SWNT, PA12/MWNT, PMMA/SWNT, PS/MWNT, PVA/SWNT, epoxy/MWNT and PC/MWNT.[3–12] Though these studies suggest encouraging results, the magnitude of reinforcement by CNT as expected from theoretical consideration is found to be limited due to the inadequate dispersion/distribution of CNT in polymer matrices and poor interfacial adhesion between CNT and polymer matrix.

Irrespective of the method of composite preparation, CNT aggregation in polymer matrices is found in most of the cases. The reasons for this lie in the strong van der Waals interactions between the tubes and the synthesis procedures often resulting in highly entangled or bundled aggregates. In context with industrial applications, melt mixing is the preferred method of composite formation. By appropriate application of shear during melt mixing CNT agglomerates may be reduced in size or disintegrated.[13]

Several studies report about different routes in order to disperse CNT more homogeneously and enhance at the same time the interfacial adhesion between the polymer matrix and the carbon nanotubes. These include the use of non-ionic surfactants, the use of amphiphilic molecules such as palmitic acid and adding functionalized CNT in CNT/polymer composites.[14–17] Poly(n-butyl acrylate) (PBA) encapsulated MWNT were reported to enhance the interfacial adhesion between PA6 and MWNT.[18] In melt-mixed composites of PA6 and modified MWNT (purified

[1] Department of Metallurgical Engineering & Materials Science, Indian Institute of Technology Bombay, Powai, Mumbai-400076, India
Fax: (+91) 22-25723480
E-mail: arupranjan@iitb.ac.in
[2] Department of Polymer Reactions and Blends, Leibniz Institute of Polymer Research Dresden, Hohe Strasse 6, D-01069 Dresden, Germany

COOH- and OH- functionalized MWNT) an increase of 115% in elastic modulus and of 124% in yield strength of PA6 was reported at 1 wt.-% MWNT level[19] whereas at 2 wt.-% MWNT elastic modulus increased by 214% and yield strength by162%. [20] It is also found that modulus and yield strength increase considerably at very low loadings (0.2 wt.-%) of functionalized MWNT. However, elongation at break decreased with increase in functionalized MWNT content.

Recently, we reported a novel approach of utilizing an interfacial reaction induced uniform dispersion of SWNT in PA12 matrix. This has been achieved by melt-mixing SMA (styrene maleic anhydride copolymer) encapsulated SWNT with PA12 which leads to better dispersion with enhanced interfacial adhesion between PA12 and SWNT as observed by enhanced dynamic mechanical moduli, improved tensile properties and changed rheological behaviour of the PA12/SWNT composites.[21]

The concept of reactive compatibilization commonly used for multiphase polymer blends has been extended in this study towards melt-mixed composites of PA6/SWNT utilizing the melt interfacial reaction between the maleic anhydride functionality of SMA and the amine end groups of PA6 with the aim to overcome the strong intertubes van der Waals interactions. Mechanical properties, morphology, rheology, and electrical conductivity have been studied.

Experimental Part

Materials and Composite Preparation

The SWNT (Buckypearls) are obtained from Carbon Nanotechnologies Inc (CNI, Houston, TX, USA) and were produced by high-pressure decomposition of carbon monoxide supported by Fe catalyst (HiPco process). As reported by the supplier, the metallic impurity level in this product is 5% and of the carbon, more than 95% is SWNT. Polyamide 6 (PA6, Durethan B29) used in this study was supplied by Bayer AG (Dormagen, Germany) in pellet form. This PA6 is an intermediate product without any nucleating agent.[22]^{1}H-NMR indicated nearly equivalence of NH_2 and COOH end groups and a degree of polymerization of about 105. Two different grades of styrene maleic anhydride copolymer (SMA, supplied by NOVA Chemicals Corporation) were used: Dylark 232 (SMA8) and Dylark 332 (SMA14) where the MA levels are 8 and 14%, respectively.

The SMA modified SWNT were prepared by dissolving appropriate amount of SMA in 50 ml tetrahydrofurane (THF) solvent, utilizing ultrasonicator aided dispersion of SWNT for 15 min and subsequently making a 'mat' by solvent removal. Unmodified SWNT were treated in the same way. The unmodified SWNT and the SMA modified SWNT based PA6 composites were prepared by melt mixing in a conical twin-screw extruder (DACA Micro Compounder) at concentrations of 1.26 and 1.5 wt.-% of SWNT at 230 °C with a rotational speed of 50 rpm for 15 min. In case of SMA modified SWNT composites, SMA concentration was varied from 0.24 to 1 wt.-%. For comparison, the mixing sequence was changed. PA6 was melt mixed with SMA 14, then in a second mixing step 1.5 wt.-% SWNT were added to PA6/SMA mixture so that the SMA concentration was 1 wt.-% in the final composite. Prior to mixing all materials were dried for 24 h at 80 °C in a vacuum oven. From the extruded strands films with a thickness of 0.35 mm were compression moulded using a Vogt press at 230 °C.

Characterization

The IR spectra were measured in transmission mode using melt films with a thickness of around 15 μm by means of the spectrometer IFS66v (BRUKER Optics, Germany). The measurement was done with a DTGS detector; a resolution of 2 cm^{-1} and with 32 scans. Before preparing the melt films all samples were dried at 80 °C under vacuum for 16 h. The melt films were prepared at 230 °C. The spectra are shown as the difference spectra of PA6/SWNT, PA6/SWNT+SMA14, and PA6/SMA14 in

which the spectrum of the pure PA6 (processed in the same way like the composites) was subtracted from the measured spectra of the reactive mixture and composites.

Melt rheological measurements were performed using an ARES oscillatory rheometer (Rheometric Scientific) at 260 °C in nitrogen atmosphere. Prior to measurements, the pure components and the extruded materials were dried for at least 1 day at 80 °C. Parallel plate geometry (plates 25 mm diameter, gap of 1 to 2 mm) was used. Frequency sweeps were carried out between 100 and 0.1 rad/s at strains within the linear viscoelastic range, which was checked for each sample. The volume resistivity was measured on compression moulded thin sheets (diameter 60 mm, thickness 0.35 mm) prepared from the strands. A Keithley electrometer model 6517 with a 8009 Resistivity Test Fixture equipped with ring electrodes was used to measure volume resistivity of the samples.

Tensile properties were measured on a Zwick Z010 tensile tester according to ISO 527-2 procedure at an extension rate of 5 mm/min on miniature dogbones (length 20 mm, parallel length 6 mm, gauge width 2 mm) punched from the pressed sheets.

Scanning electron microscopic (SEM) investigation was performed using FEI Quanta 200 with sample sputtering on tensile fractured samples.

Results and Discussion

Interfacial Reaction

In our approach we assume that the SMA copolymer forms a layer around the carbon nanotube surface after the solvent treatment. Because of dispersive interactions between the aromatic groups of the styrene and the SWNT we expect that the styrene part of the copolymer is located and fixed at the SWNT surface. Thus, the maleic anhydride groups should be available for the interfacial reaction with the polyamide end groups forming imide groups. The anhydride-amine reaction was shown in literature as one of the most effective reactions in polymer blend compatibilization.[23] It is very fast and can be accomplished within short melt mixing time, which is the reason for selecting this reaction for our new approach. Using infrared spectroscopy we followed the reaction. Figure 1 shows difference spectra of different samples. PA6/SMA14 and

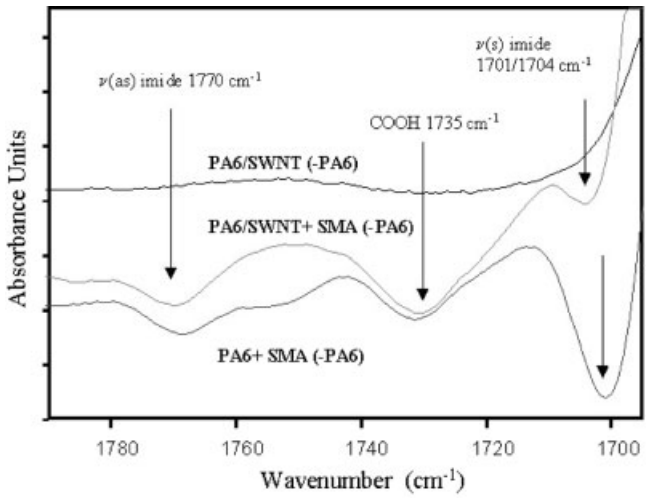

Figure 1.
IR analysis: difference spectra of PA6+SMA14 (SMA14 = 1 wt.-%), PA6/SWNT (SWNT = 1.5 wt.-%) and PA6/SWNT+SMA (SWNT = 1.5 wt.-%, SMA14 = 1 wt.-%) composites, spectrum of pure PA6 is subtracted.

PA6/SWNT+SMA14 show the bands typical of the imide group (ν(as) at 1770 cm^{-1} and ν(s) at 1701/1704 cm^{-1}). In the difference spectrum of PA6/SWNT these bands are absent. Thus, the presence of the imide groups in the IR difference spectrum clearly indicate that the intended reaction between the NH_2 end groups of the PA6 and the anhydride groups of the SMA took place during melt mixing of the SMA encapsulated SWNT with PA6. In addition, unreacted COOH end groups can be related to the peak at 1735 cm^{-1}.

DC Electrical Resistivity and Rheological Characterization

In order to follow the state of nanotube percolation within the nanocomposites, electrical resistivity measurements and melt rheological characterization are suitable methods. Even if in HiPco material only about 33% of the tubes have metallic character [24] we can expect that each bundle will contain enough metallic tubes to act as conductor in the insulating matrix. Due to the high aspect ratio, SWNT are known to form conductive nanocomposites already at very low loadings. Electrical measurements can be used as a good criterion for geometrical percolation, even if electrical percolation does not perfectly represent the geometrical percolation, since small distances in the range of 5–10 nm within the conducting elements are still possible to allow electron hopping (assuming that this mechanism apply to our system). Interestingly, electrical resistivity measurements on the composites with 1.26 wt.-% and 1.5 wt.-% SWNT revealed that in these composites SWNT percolation could not be reached. We have to assign this to the insufficient distribution and dispersion of the untreated SWNT material within the PA6 matrix. Electrical volume resistivity values were measured to be in the same range like PA6 (E13 Ω cm). However, in the composites with 1 wt.-% SMA encapsulated SWNT, electrical resistivity was obtained in the range of E06 Ω cm indicating the existence of a percolating network of the encapsulated SWNT. Thus, we can conclude that the SMA surface layer was thin enough to allow electron hopping between the SWNT bundles. On the other hand, this result shows that the dispersion of the nanotubes has been improved as compared to the untreated SWNT and the actual aspect ratio of the SWNT is increased by having lower number of tubes in the bundles. During the THF solvent treatment step much better homogeneity of the SMA-SWNT dispersions could be observed as compared to the SWNT dispersions indicating an emulsifying effect of the SMA copolymer. Interestingly, the composite of SWNT with premixed PA6/SMA also showed conductivity (resistivity values in the range E06 Ω cm) indicating a better SWNT dispersion as compared to PA6 with SWNT.

In addition, oscillatory melt rheology was used in order to check if a percolated network can be detected in the composites with encapsulated SWNT. It was shown in literature that the values of complex viscosity η^* and storage modulus G′ especially at low frequencies are sensitive to the formation of nanofiller overstructures. In some recent papers it was shown that electrical percolation and rheological percolation seem to reveal not exactly the same phenomena. Rheological percolation was observed at lower CNT concentrations than electrical since it reflects some kind of combined network between the CNT and the polymer chains.[25,26] The complex viscosity and the storage modulus of PA6 and PA6/SWNT composites are plotted as a function of angular frequency in Figure 2. Pure extruded PA6 shows Newtonian behaviour at low frequencies with a zero shear viscosity of 240 Pa s. SMA14 copolymer shows non-Newtonian behaviour at low frequency in the complex viscosity versus frequency plot. The addition of SWNT to PA6 leads to a significant increase in complex viscosity as compared to pure PA6. At low frequency, a deviation from the Newtonian behaviour can be observed seeing as an increase in viscosity values by lowering the frequency. Also in the G′ vs. frequency behaviour especially at

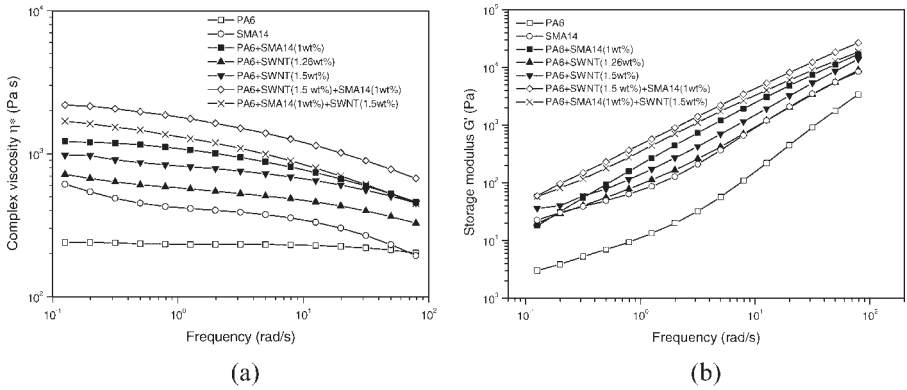

Figure 2.
Melt rheological behaviour of PA6 and different composites at 260 °C, (a) complex viscosity versus vs. frequency, (b) storage modulus vs. frequency.

1.5 wt.-% SWNT a plateau starts to develop. The addition of SMA to PA6 leads to much higher viscosity values indicating the reaction discussed above which is a bulk reaction in this case. The zero shear viscosity is about five times that of PA6. As shown before, the encapsulation of SWNT by the SMA copolymer enhances the dispersion of the nanotubes and leads to an interfacial reaction, therefore these composites show higher viscosity and moduli as compared to those without modifier. Interestingly, the sequence of mixing plays a role on the melt rheological properties of the composites. When introducing SWNT in the PA6/SMA premixture, values of complex viscosity and storage modulus are lower as compared to incorporation of encapsulated SWNT into PA6. We attribute this mainly to the better dispersion and specific interaction at the interface between SWNT and PA6 when using encapsulated SWNT in PA6, both leading to the increase in viscosity and modulus. When incorporating SWNT into the PA6/SMA premixture, the main effect consists in the higher melt viscosity of the matrix leading to higher shear forces favourable for distribution and dispersion of the SWNT. In addition, we may assume a lower interfacial tension between PA6/SMA and SWNT as compared to PA6 and SWNT.

Tensile Properties

Due to the interfacial reaction shown before we expect that during tensile deformation the presence of SMA copolymer facilitates the stress transfer from the matrix (PA6) to the SWNT, thus leading to enhanced mechanical properties. In this system, changes in crystallinity are only marginal so that differences in the stress-strain behaviour can be related mainly to changes in SWNT dispersion and interfacial adhesion.[27]

Figure 3 shows representative stress-strain curves of different compositions of PA6, SWNT and SMA together with pure PA6. It is evident from Figure 3 that all the samples exhibit a pronounced yield point followed by cold drawing and strain hardening. When adding 1.5 wt.-% SWNT to PA6, an increase in tensile modulus by 15% and stress at yield by 11% occurs, however, elongation at break is reduced drastically.[27] Simultaneously, also stress at break is reduced. The stress-strain behaviour of the PA6 seems to be influenced by the presence of the loose network-like structure of SWNT (see Figure 5a), which hinders the cold drawing process and/or by the existence of agglomerates acting as defects. In addition to this, the lack of adequate interfacial adhesion between PA6 and SWNT may be responsible for lower ultimate tensile strength

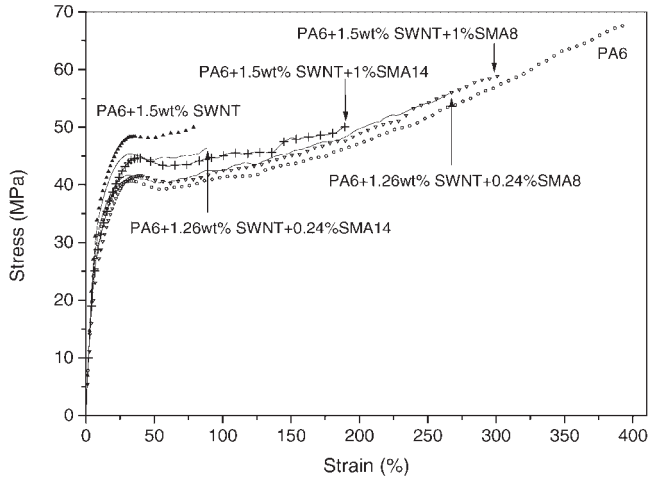

Figure 3.
Representative tensile stress-strain curves of different composites.

and lower elongation at break as compared to pure PA6.

When adding SWNT encapsulated by SMA8 into PA6, values of stress at yield and the stress levels after the yield point are only slightly higher than those of PA6. These stress values are significantly lower than those of the composite with untreated SWNT. On the other hand, elongation at break increases significantly as compared to the PA6/SWNT composites and therefore the composites reach higher values of tensile strength. However, elongation at break is still lower than that of pure PA6. Both composites with SWNT encapsulated by SMA14 show higher yield stress and stress levels after the yield point than the composites with SMA8 modified SWNT (but reduced values as compared to PA6/SWNT). On the other hand, elongations at break are lower than that of SWNT encapsulated by SMA8. For both SMA types, higher SMA loading leads to higher values of elongation at break. This observation may be explained by a more efficient load transfer with increase in SMA concentration, which facilitates plastic deformation. The increased tensile modulus and yield stress with the incorporation of SMA14 (as compared to SMA8) may be related to higher entanglements at the interface, which is a result of a more pronounced interfacial reaction in the presence of SMA14.

Morphology of Tensile Fractured Surfaces

Scanning electron micrographs of fractured surfaces as shown in Figures 4–6 were used to get information about the kind of fracture of the nanocomposites, the state of dispersion of the SWNT, and the characterization of interfacial adhesion between SWNT and PA6 matrix.

Low magnification images of PA6 show the presence of shear bands (Figure 4a), which is an indication of ductile failure as reported earlier.[28] In contrast, composites of PA6/SWNT did not show any sign of shear bands (Figure 4b, 5a). Extensive cracks are observed in the entire fracture surface. At higher magnification, it is observed that SWNT bundles appeared as a loose network-like structure along with aggregated bundles of SWNT (Figure 5a). No breakage of the tubes could be found, rather the 'weave-like bundles' disentangled during tensile deformation. It appears from the fractured surfaces that in case of PA6/SWNT composites, catastrophic failure of the matrix leads to extensive cracks and SWNT could not participate in the load transfer process

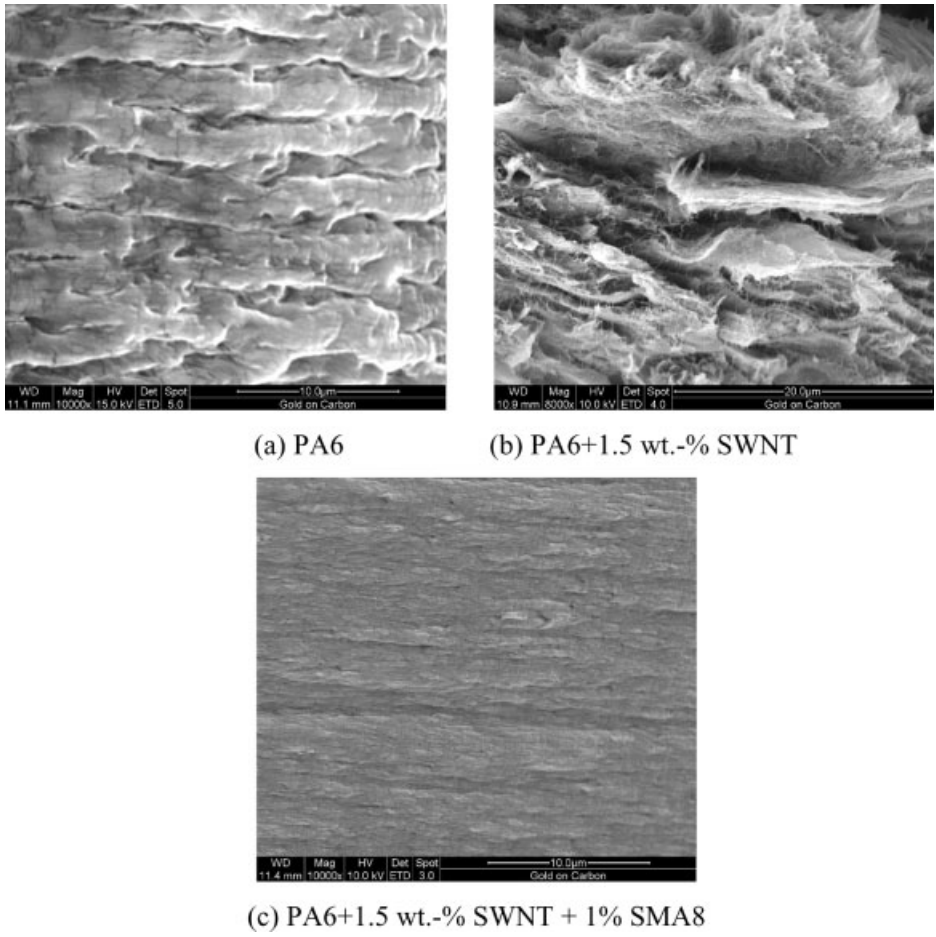

Figure 4.
Scanning electron micrographs of tensile fractured surfaces showing shear bands in (a) and (c), and catastrophic failure in (b).

due to the absence of any interfacial adhesion between PA6 and SWNT.

Composites of SMA modified SWNT show the presence of shear bands (Figure 4c) in the crack-propagating zone and highly adhered SWNT in PA6 matrix (Figure 5b, 6b) in the crack-initiating zone. A similar kind of morphological feature was reported in functionalized MWNT based PA6 composites, where aligned tubes were found to bridge across the micro-cracks of crack widths more than 10 μm.[20]

It is evident that the SMA modification leads to less entangled SWNT bundles in PA6 matrix if we compare Figures 5a and 5b. One can even observe the reduction of SWNT bundle diameter in Figure 5b, which indicates better dispersion of SWNT in presence of SMA copolymer. Figure 6a shows that several micron long SWNT bundles stretch between one part of the matrix to the other part and were found to bridge the crack in SMA modified PA6/SWNT composites. This indicates efficient load transfer during deformation due to the enhanced interfacial adhesion. A closer inspection of fractured surfaces of SMA modified PA6/SWNT composites confirms the encapsulation process since a thick layer around SWNT bundles was found, which is evident even at lower magnification (Figure 6b).

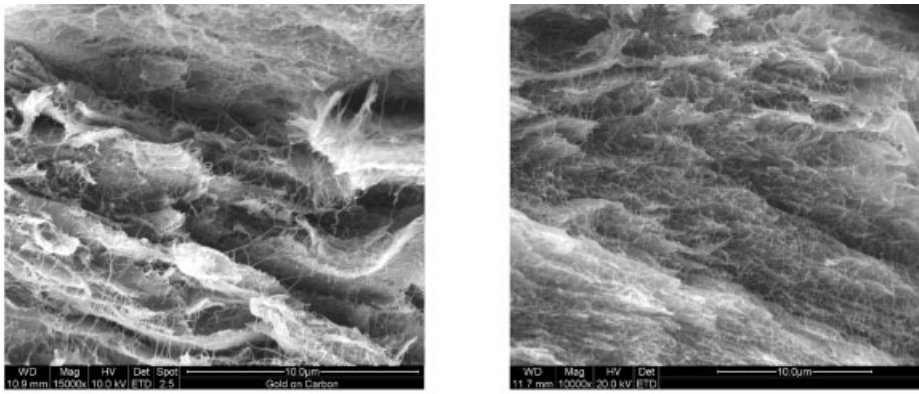

Figure 5.
Scanning electron micrographs of tensile fractured surfaces showing better dispersion and interfacial adhesion between PA6 and SWNT in presence of SMA.

Summary and Conclusions

Styrene maleic anhydride copolymer (SMA) encapsulated single wall carbon nanotubes (SWNT) are melt-mixed with polyamide 6 (PA6) utilizing the concept of reactive compatibilization using an interfacial reaction between the anhydride functionality of SMA and the amine end groups of PA6. The aim was to disperse SWNT more homogeneously in the matrix and to enhance the interfacial adhesion between PA6 and SWNT.

SMA was found to act as a reactive compatibilizer between PA6 and SWNT as evident from IR spectroscopy. The encapsulation of SWNT by SMA copolymer was shown to enhance the interfacial adhesion between PA6 and SWNT as observed from the tensile fractured surfaces of PA6/SWNT+SMA composites. This observation is supported by increased values of elongation at break of the composites with SMA modified SWNT as compared to composites with unmodified SWNT. For

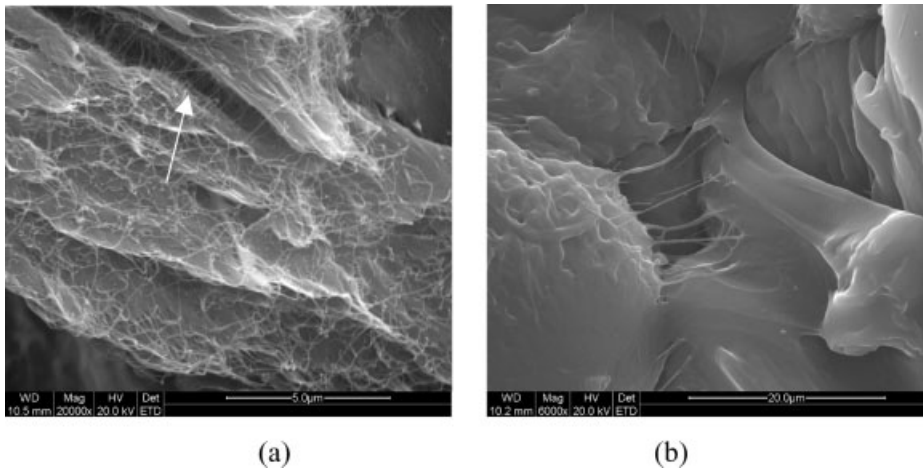

Figure 6.
Scanning electron micrographs of tensile fractured surfaces of PA6 + 1.5 wt.-% SWNT + 1% SMA8 showing stretched SWNT bundles in (a) and encapsulated polymer layer around SWNT bundles in (b).

composites with 1.5 wt.-% SWNT and 1% SMA also the ultimate tensile strength was enhanced as compared to composites with 1.5 wt.-% SWNT.

Overall, it can be concluded that the SMA encapsulation of SWNT leads to a partial wrapping of a polymer layer (SMA and reactively coupled PA6 chains) on the SWNT bundles, which is evident from fractured surface morphology. On the other hand, the composites with encapsulated SWNT showed conductivity, indicating that such wrapping does not completely prevent touching of SWNT within a certain distance necessary for electron transport. The resistivity values and the rheological results together with SEM observations indicate that the SWNT dispersion is much better in case of encapsulated SWNT. However, the formation of a SWNT network and the existence of SWNT agglomerates seem to influence the typical deformation behaviour of the PA6 matrix significantly since the PA6 is hindered in its typical cold drawing and strain hardening behaviour.

In summary, the mechanical properties of these composites are related to a complex interplay between the extent of encapsulation and the extent of reaction at the interface leading to changed interfacial adhesion, the state of SWNT dispersion, and the state of percolation of the SWNT in the matrix. More investigations are needed in order to optimize the encapsulation process.

Acknowledgements: We would like to acknowledge financial assistance of the Leibniz Institute of Polymer Research Dresden by providing fellowships to one of the authors (ARB) during his post-doctoral stays. We thank Bayer AG for giving permission to use the PA6 in this study. In addition, we are grateful to Dr. Dieter Fischer (IPF Dresden) for IR measurements and to Vivek Pancholi (OIM-SEM National Facility, IIT Bombay) for assistance in SEM investigation.

[1] J. P. Salvetat, G. A. D. Briggs, J. M. Bonard, R. R. Bacsa, A. J. Kulik, T. Stöckli, N. A. Burnham, L. Forró, *Phys. Rev. Lett.* **1999**, *74*, 3803.
[2] M. S. Dresselhaus, G. Dresselhaus, Ph. Avouris, "*Carbon nanotubes: synthesis, structure, properties, and applications*", Springer-Verlag, Germany, 2001.
[3] S. Kumar, T. D. Dang, F. E. Arnold, A. R. Bhattacharyya, B. G. Min, X. Zhang, R. A. Vaia, C. Park, W. W. Adams, R. H. Hauge, R. E. Smalley, S. Ramesh, P. Willis, *Macromolecules* **2002**, *35*, 9039.
[4] L. Valentini, J. Biagiotti, J. M. Kenny, S. Santucci, *J. Appl. Polym. Sci.* **2003**, *87*, 708.
[5] B. P. Grady, F. Pompeo, R. L. Shambaugh, D. E. Resasco, *J. Phys. Chem. B* **2002**, *106*, 5852.
[6] A. R. Bhattacharyya, T. V. Sreekumar, T. Liu, S. Kumar, L. M. Ericson, R. H. Hauge, R. E. Smalley, *Polymer* **2003**, *44*, 2373.
[7] J. K. W. Sandler, S. Pegel, M. Cadek, F. Gojny, M. van Es, J. Lohmer, W. J. Blau, K. Schulte, A. H. Windle, M. S. P. Shaffer, *Polymer* **2004**, *45*, 2001.
[8] R. Haggenmueller, A.G. Gommans, A. G. Rinzler, J.E. Fischer, K.I. Winey, *Chem. Phys. Lett.* **2000**, *330*, 219.
[9] L. S. Schadler, S. C. Giannaris, P. M. Ajayan, *Appl. Phys. Lett.* **1998**, *72*, 3842.
[10] M. S. P. Shaffer, A. H. Windle, *Adv. Mater.* **1999**, *11*, 937.
[11] J. Sandler, M. S. P. Shaffer, T. Prasse, W. Bauhofer, K. Schulte, A. H. Windle, *Polymer* **1999**, *40*, 5967.
[12] P. Pötschke, A. R. Bhattacharyya, A. Janke, H. Goering, *Comp. Interf.* **2003**, *10*, 389.
[13] D. W. Ferguson, E. W. S. Bryant, H. C. Fowler, ESD thermoplastic product offers advantage for demanding electronic applications, *SPE ANTEC* 1998, 1219.
[14] X. Gong, J. Liu, S. Baskaran, R. D. Voise, J. S. Young, *Chem. Mater.* **2000**, *12*, 1049.
[15] S. Barrau, P. Demont, E. Perez, A. Peigney, C. Laurent, C. Lacabanne, *Macromolecules* **2003**, *36*, 9678.
[16] C. A. Mitchell, J. L. Bahr, S. Arepalli, J. M. Tour, R. Krishanamoorti, *Macromolecules* **2002**, *35*, 8825.
[17] C. Velasco-S., A. L. Martinez-H., F. T. Fisher, R. Ruoff, V. M. Castano, *Chem. Mater.* **2003**, *15*, 4470.
[18] H. Xia, Q. Wang, G. Qiu, *Chem. Mater.* **2003**, *15*, 3879.
[19] W. D. Zhang, L. Shen, I. Y. Phang and T. Liu, *Macromolecules* **2004**, *37*, 256.
[20] T. Liu, I. Y. Phang, L. Shen, S. Y. Chow, W. D. Zhang, *Macromolecules* **2004**, *377*, 214.
[21] A. R. Bhattacharyya, P. Pötschke, M. Abdel-Goad, D. Fischer, *Chem. Phys. Lett.* **2004**, *392*, 28.
[22] S. H. Jafari, P. Pötschke, M. Stephan, H. Warth, H. Alberts, *Polymer* **2002**, *43*, 6985.
[23] U. Sundararaj, C. W. Macosko, *Macromolecules* **1995**, *28*, 2647.
[24] S. M. Bachilo, M. S. Strano, C. Kittrell, R. H. Hauge, R. E. Smalley, R. B. Weisman, *Science* **2002**, *298*, 2361.
[25] F. Du, R.C. Scogna, W. Zhou, S. Brand, J.E. Fischer, K.I. Winey, *Macromolecules* **2004**, *37*, 9038.
[26] M. Abdel-Goad, P. Pötschke, *Journal of Non-Newtonian Fluid Mechanics* **2005**, *128*, 2.
[27] A. R. Bhattacharyya, P. Pötschke, L. Häußler, D. Fischer, Reactive Compatibilization of Melt-Mixed PA6/SWNT Composites: Mechanical Properties and Morphology, *Macromolecular Chemistry and Physics*, **2005**, *206*, 2084.
[28] A. R. Bhattacharyya, S. N. Maiti, A. Misra, *J. Appl. Polym. Sci.* **2002**, *85*, 1593.

